Analysis and Simulation of Dynamic Performance of PMU According to IEEE C37.118.1-2011 Standard

Marcelo N. Agostini
marcelo.agostini@reason.com.br

Adriano O. Pires
adriano.pires@reason.com.br

Sérgio L. Zimath
sergio.zimath@reason.com.br

Lucas B. de Oliveira
lucas.oliveira@reason.com.br

Paulo R. F. de Souza
paulo.de-souza@reason.com.br

GE Grid Solutions
Phone: +554821080300
Rua Delminda Silveira 855, 88025-500
Florianopolis, SC, Brazil

ABSTRACT

With the growth in the number of PMUs in the electrical system, the discussion and understanding of performance requirements required in IEEE standard C37.118.1-2011 and its addendum IEEE C37.118.1a-2014 is of fundamental importance for the future specification, operation and maintenance of future interconnected power grids. This paper presents an analysis of two different algorithms for calculating synchrophasors in accordance with limits and test methods proposed in the IEEE standard. Results are presented using a hybrid simulation platform, in which the algorithms are implemented in a real PMU.

KEYWORDS

PMU, Phasor Measurement, PMU standard, IEEE C37.118, PMU certification, WAMS

1. INTRODUCTION

The increase in operating complexity of power systems has required the constant improvement of its monitoring and control instruments, both real-time and offline. This demand has led to the development of innovative technologies, scenario in which stands the wide area measurements. Wide area measurement systems (WAMS) are formed basically by phasor measurement units (PMU) installed in substations, which measure voltage and current synchrophasors and send them to phasor data concentration systems (PDC) usually installed operating centers. All the PMUs are synchronized from a common time base, usually through the GPS system. This ensures that a single set of synchrophasors measured by all devices on a particular instant of time represent an instantaneous operating point of the power system. Measuring rates of the same order of magnitude of the electrical system frequency allows the monitoring of the dynamics of these systems.

WAMS are being developed in many countries. In Brazil, a single synchronized phasor measurement system is being implemented for the National Interconnected System, called SMSF-SIN. This process has been led by the National Electric System Operator (ONS). Deployment initiatives of other WAMS can be identified in electrical transmission and generation agents at different stages of development. The pioneering project for wide area measurement in South America was led by the Federal University of Santa Catarina (UFSC), with the participation of Reason Technology. The project named MedFasee, installed PMUs in 23 partner universities in the low voltage electrical system, covering the five geographic regions of Brazil.

Alongside the various initiatives that deal with the development of phasor measurement technology, both in relation to monitoring equipment and the applications of phasor data in monitoring and operation of electrical systems, some issues regarding precision and accuracy of these measures have been the focus of discussions. The use of phasors, a representation of a sine wave with constant frequency (steady state), to depict the actual operating conditions of electrical systems when the frequency of the system is not constant, raises discussions about the quality and applicability of these measurements. One point of discussion, for instance, is the comparability and interoperability between PMUs from different manufacturers, in light of possible divergent interpretations of how to compute synchrophasors.

The phasor measurement is discussed in the IEEE C37.118 standard. In 2011 this standard was reviewed and split in two parts, C37.118.1-2011 and C37.118.2-2011. The first part deals with the

measurement of synchrophasors itself, and the second data communication between devices in a phasor measurement system. Additionally, in part one of the standard, a set of steady-state and dynamic performance tests were added, including the definition of error limits for the compliance check of PMUs. Some of these limits and some testing procedures were reviewed and adjusted recently in the IEEE C37.118.1a-2014 addendum.

With the growing number of PMUs installed in the electrical system, the discussion and understanding of the performance required in the new version of the standard, as well as its recent addendum, is of fundamental importance to the proper specification and proper operation and maintenance of WAMS. Some proposed tests have performance limits that compete with each other, limiting significantly the response allowed for the PMUs, and therefore requiring accurate performance of internal algorithms for synchrophasors calculation. PMUs that have adequate performance in a given set of tests may not repeat the same performance in other types of testing.

This paper presents two distinct algorithms Synchrophasors calculation. Some aspects related to tests and limits proposed in the IEEE standard C37.118.1-2011 and its addendum IEEE C37.118.1a-2014 are described and discussed, especially regarding the frequency response of the PMU. The complementarity between tests is discussed and particular performance characteristics of each synchrophasor computation algorithm are presented per test type. Results are showed using a hybrid simulation platform, in which the algorithms are implemented on a real PMU equipment.

2. BAND REJECTION AND MODULATION

With respect to the frequency response of the PMU, the synchrophasor standard proposes band rejection (out-of-band interference, or OOB) and modulation (measurement bandwidth) tests. The first aims to verify the capacity of the PMU to reject signals outside the measurement frequency range, as signals outside this range could cause aliasing in measurements. The frequency bandwidth f of allowed signals is given by:

$$|f - f_N| < \frac{F_S}{2} \qquad (01)$$

where f_N is the nominal frequency, F_S is synchrophasors publishing rate, and $\frac{F_S}{2}$ is the respective Nyquist frequency. For example, at the rate of 60 FPS, the passband lies between 30 Hz and 90 Hz. Signals outside this range, below 30 Hz and above 90 Hz, must be rejected by the PMU.

The goal of the modulation test, however, is to check the PMUs ability to correctly measure low-frequency oscillations, which are produced by electromechanical oscillations in the power system. In this test, both amplitude (module) and phase (angle) of the PMU input signals are modulated with low-frequency carrier signals whose frequency depends on the PMU's transmission rate. The test is performed by checking whether the modulating signals are correctly presented in the synchrophasors measured by PMU.

Considering an input signal with a nominal frequency $f_N = 60$ modulations in module and/or angle with frequency $f_{mod} = 0{,}7$ or $f_{mod} = 1{,}2$ for example, produce spectral components at $(f_N \pm f_{mod})$ (59.3 Hz and 60.7 Hz or 58.8 Hz and 61.2 Hz, respectively). This is equivalent to having interference signals with frequencies $(f_N \pm f_{mod})$ in the input signal, as shown in Figure 1.

Observing the effects in the frequency domain, modulation and OOB tests may be considered complementary. The first requires the PMU to reject signals whose spectral components are located below $\left(f_N - \frac{F_S}{2}\right)$ and above $\left(f_N + \frac{F_S}{2}\right)$. Meanwhile the second requires that the modulation signals with spectral components $(f_N \pm f_{mod})$, with f_{mod} dependent on the transmission rate, be measured by PMU with low errors. Table 1 shows the "band allowance" between the frequency bands of the modulation and OOB tests considering the nominal frequency $f_N = 60$ Hz, i.e. the bandwidth allowed for the filter to change from rejecting to permissible state and vice versa.

It can be seen that the band allowance decreases considerably as the transmission rate of phasors is reduced. This shows that the selectivity of the PMU algorithm should increase drastically as the rate of transmission decreases.

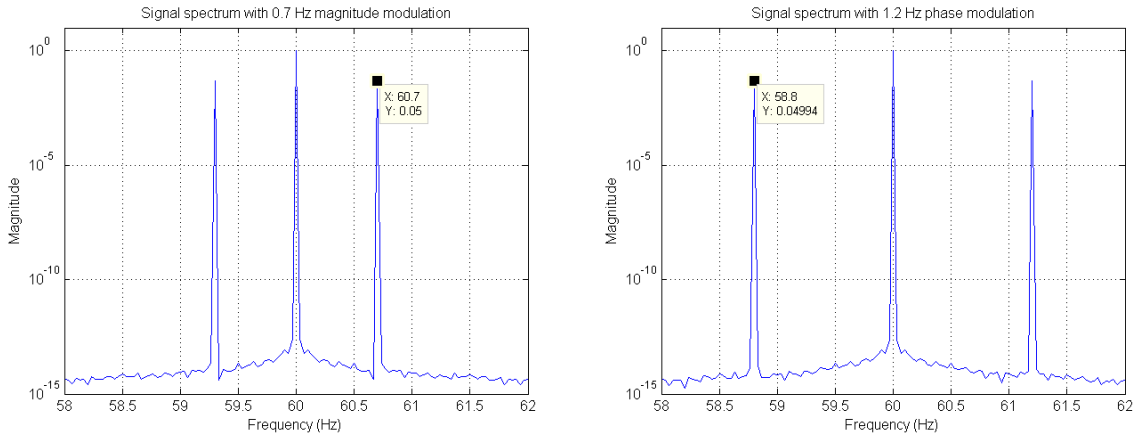

Figure 1: Relationship between modulation and the modulated signal spectrum

Table 1: Band allowance between OOB and Modulation ($f_N = 60$ Hz)

F_S (FPS)	$f_{mod\ max}$ (Hz)	$\left[f_N - \frac{F_S}{2}\right]$ (Hz) (*reject below*)	$[f_N - f_{mod\ max}]$ (Hz) (*allow above*)	$\left[\frac{F_S}{2} - f_{mod\ max}\right]$z) (*band allowance*)
60	5	$f \leq 30$; $f \geq 90$	$55 \leq f \leq 65$	25
30	5	$f \leq 45$; $f \geq 75$	$55 \leq f \leq 65$	10
20	4	$f \leq 50$; $f \geq 70$	$56 \leq f \leq 64$	6
15	3	$f \leq 52{,}5$; $f \geq 67{,}5$	$57 \leq f \leq 63$	4,5
12	2,4	$f \leq 54$; $f \geq 66$	$57{,}6 \leq f \leq 62{,}4$	3,6
10	2	$f \leq 55$; $f \geq 65$	$58 \leq f \leq 62$	3

3. ALGORITHMS FOR CALCULATING SYNCHROPHASORS

In this work two algorithms were considered for calculating synchrophasors, both based on the Discrete Fourier Transform (DFT). The basic distinction between the algorithms is the data window strategy.

3.1. DISCRETE FOURIER TRANSFORM

The Discrete Fourier Transform (DFT) is represented by equation (02):

$$\bar{X}_h = \sum_{n=0}^{N-1} x_n \left(\cos \frac{2\,\pi\,h\,f_0\,n}{f_{acq}} - i \sin \frac{2\,\pi\,h\,f_0\,n}{f_{acq}} \right) \qquad (02)$$

where:

$h \rightarrow$ integer order of the harmonic frequency

$\bar{X}_h \rightarrow$ phasor relative to the harmonic of order h

$N \rightarrow$ window size given in number of samples

$x_n \rightarrow$ nth sample

$f_0 \rightarrow$ fundamental frequency of the DFT

$f_{acq} \rightarrow$ acquisition frequency

Typically in PMUs the f_{acq} is fixed and synchronized, ensuring that the measured phasors have the same time base. It is also worth pointing out that f_{acq} is an integer multiple M of the nominal frequency f_N of the electrical system. The relationship between f_{acq} and f_N is given in points per cycle (ppc). For example, a PMU operating with $f_N = 60$ Hz with $M = 256$ ppc has $f_{acq} = 15.360$ Hz. It is convenient to

use windows sizes that are multiples of the sampling cycle, $N = kM$. The relationship between f_{acq} and the window size N determines f_0, according to equation (03).

$$f_0 = \frac{f_{acq}}{N} = \frac{f_N\, M}{k\, M} = \frac{f_N}{k} \tag{03}$$

To calculate the phasor in an electrical system only f_N is of interest. Furthermore, as the harmonic frequency $f_h = h\, f_o$, then it is only necessary to calculate the phasors of the component $\bar{X}_h$ for $h = k$.

It should be noted that the instantaneous frequency of the electrical system is not equal to the nominal frequency. This oscillation in frequency is due to the constant action of the control loops in the search for balance between load and generation. As the period of the waveform measurement is not exactly equal to the size of the DFT window, a phenomenon called spectral leakage occurs. Spectral leakage is one of the sources of errors that may compromise the accuracy of phasor estimation. To mitigate its effects, window functions which aim to assign different weights to the data distributions used in DFT are commonly used.

3.2. WINDOW FUNCTIONS

In this work we use two types of windows functions: Hann and Flat Top. In the Hann window, the w_n weights of each sample x_n in the DFT are given by (04):

$$w_n = \frac{1}{2}\left(1 - \cos\frac{2\,\pi\, n}{N}\right) \quad ; \quad n = 0\,,1\,,\ldots,N-1 \tag{04}$$

In the case of Flat Top windows, the weights are given by (05):

$$w_n = \sum_{j=0}^{J} a_k \cos\frac{2\,\pi\, j\, n}{N} \quad ; \quad n = 0\,,1\,,\ldots,N-1 \tag{05}$$

in this paper we have set $J = 4$ (Flat Top with 5 terms) and coefficients a_k given in [05].

In Figure 2 we can see a comparison between Hann and Flat Top 5 windows, assuming $h = k = 1$ and $f_N = f_0 = 60$ Hz. On the Flat Top window function, samples closer to the center of the window are prioritized, as its frequency spectrum presents a flatter gain profile near the frequency of the harmonic of interest ($f_h = 60$ Hz). The cutoff of the first lobe for this function lays on the fifth bin, $(f_h + 5\, f_0)$. In comparison, for the Hann window, the cutoff of the first lobe happens in the second bin, $(f_h + 2\, f_0)$. The attenuation of the second lobe onwards is larger on the Flat Top 5 than in the Hann window (Figure 2b), indicating its greater selectivity.

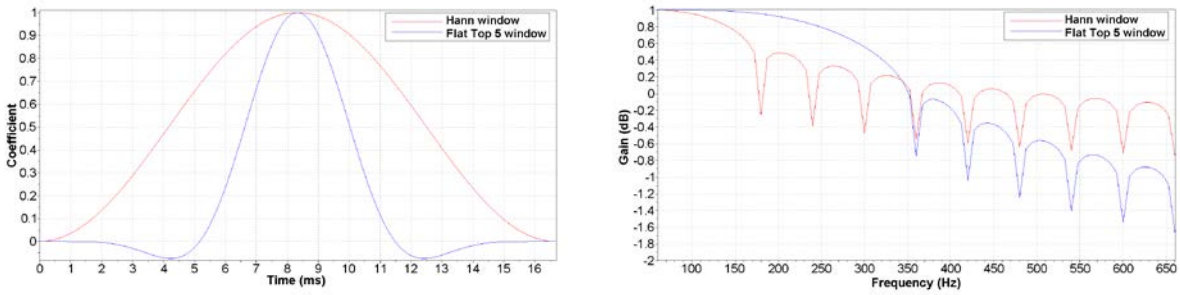

(a) Time domain (b) Frequency domain

Figure 2: Comparison between the types of window functions

3.3. APLICATION OF WINDOW FUNCTIONS IN THE ALGORITHMS

For the first algorithm considered in this paper a Hann window was used. Its window size and the DFT fundamental frequency f_0 were adjusted according to the instantaneous frequency of the electrical system f_{in}. Frequency is estimated at each computation step from the first derivative of the angle of the positive sequence voltage of preliminary synchrophasors. These preliminary synchrophasors are calculated using a DFT with the window function set to a sampling cycle and a fundamental frequency equal to the nominal frequency of the power system. The estimated frequency is then used to adjust the window size of the main DFT algorithm, which calculates the actual PMU synchrophasors. A resampling process is used to assist with the window size adjustment. The frequency subsequently recalculated, again derived from the angle of the positive sequence voltage PMU synchrophasors.

Considering $f_N = 60$ Hz and $f_{in} \approx f_N$, a window with $h = 4\,\frac{f_N}{F_S}$ and $k = 4\,\frac{f_{in}}{F_S}$ is used, in order to correctly place the cutoff frequencies for the OOB. Assuming the transmission rate $F_S = 60$ FPS, $h = 4$, and $k \approx 4$, yields a DFT fundamental frequency of $f_0 \approx 15$ Hz, whose 4th harmonic frequency is $f_h \approx 60$ Hz. Such parameters thus position the first lobe centered at f_h, with cutoff frequencies in ≈ 30 Hz and ≈ 90 Hz.

These values vary with each transmission rate. For $F_S = 10$ FPS, for instance, $h = 24$, $k \approx 24$, $f_0 \approx$ 2,5 Hz and $f_h \approx 60$ Hz, yielding cutoff frequencies in ≈ 55 Hz and ≈ 65 Hz. The frequency of the synchrophasor of interest, $\bar{X}_h$, calculated by DFT, may be considered equal to the nominal frequency so that $f_h \approx f_{in}$. This assumption holds as the window size N should be rounded to an integer number of samples when $N = kM$ is computed.

With this approach, the number of points used in the DFT calculation for each cycle varies according to the instantaneous frequency of the electrical system. It is also necessary to recalculate the trigonometric terms of the DFT for each frequency. Considering such calculations are onerous in terms of computational performance for embedded systems, lookup tables are typically used. These tables hold pre-calculated values of the sines and cosines for an expected frequency variation range. In this work, a 10 Hz frequency range was used (55 Hz to 65 Hz) in steps of 0.0025 Hz (4000 rows).

For the second algorithm a Flat Top 5 window with a fixed size was utilized, tuned to the nominal frequency of the electrical system. The instantaneous frequency is estimated at every computation step, using a DFT with a fixed window size and nominal frequency, like in algorithm 1. The data sampled by the device are applied directly to the window, without resampling or recalculating the trigonometric terms of the DFT. After calculating the preliminary phasors through the DFT, an 8th order polynomial is used for the correction of such phasors with the instantaneous frequency information. The frequency is then recalculated, derived from the angle of the positive sequence voltage corrected synchrophasors. There is a linear frequency correction based on the instantaneous frequency variation rate to ensure measurement performance under a dynamic regime, even with considerable number of cycles (k) in the DFT window.

Considering $f_N = 60$ Hz, a window with $h = k = 10\,\frac{f_N}{F_S}$ is designed. For the transmission rate $F_S = 60$ FPS, $h = k = 10$, yielding a DFT fundamental frequency of $f_0 = 6$ Hz and a harmonic frequency of $f_h = 60$ Hz, positioning the first lobe cutoff frequencies exactly at 30 Hz and 90 Hz. These values vary according to each transmission rate, reaching $h = k = 60$, $f_0 = 1$ Hz and $f_h = 60$ Hz for $F_S = 10$ FPS, with cutoffs in 55 Hz and 65 Hz.

Algorithm 2 requires a greater window size than algorithm 1 for the correct positioning of the cutoff frequencies of the first lobe in the spectrum. Its higher selectivity, however, allows a more effective band rejection than that of algorithm 1. This response can be observed in Figure 3, in which the frequency spectra of the two window functions applied to algorithms 1 and 2 are shown, respectively, at rates of 60 FPS and 10 FPS. Gains were normalized for a better comparison. The cutoff frequencies of each algorithm may be observed for each transmission rate. Also noticeable are the reduction in the band allowance (Table 1) as the phasors transmission rate is reduced.

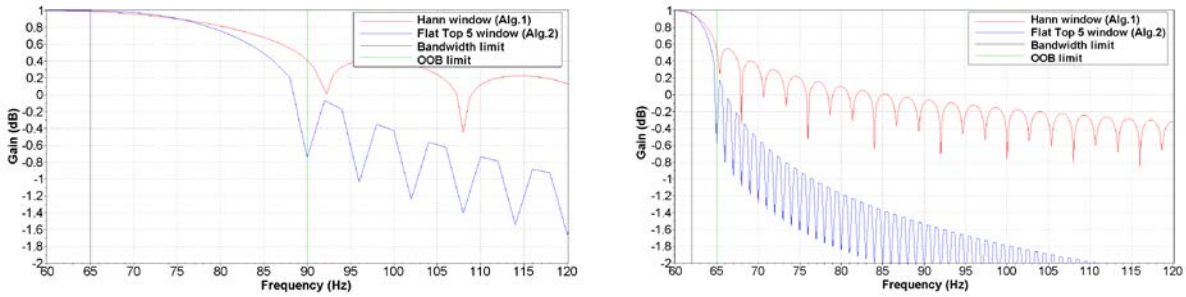

(a) 60 FPS (b) 10 FPS

Figure 3: Application of window functions to the synchrophasors calculation algorithms

4. TESTS AND RESULTS

Simulation tests were carried out according to standard IEEE C37.118.1-2011, and its addendum IEEE C37.118.1a-2014. For these tests a hybrid simulation platform was used, as shown in Figure 4.

The values of the instantaneous samples of the reference signal (waveform) in each test were generated by a personal computer and sent to the PMU. At the PMU equipment level, these values were used for the internal calculation of synchrophasors as if they were originated in their acquisition system. The synchrophasors were sent back to the PC via messages on IEEE C37.118.2-2011 format through the Ethernet network. The synchrophasors were compared with reference values, and TVE, FE and RFE errors calculated.

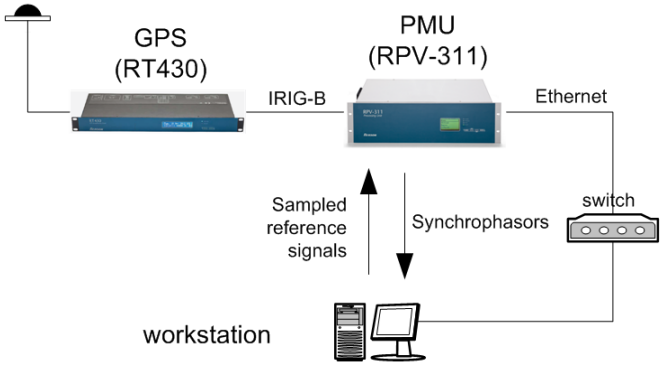

Figure 4: Hybrid simulation platform

All tests proposed in the synchrophasors standard were realized for the two algorithms mentioned above, both for static and dynamic conditions. For simplicity, this paper presents a subset of results consisting of tests in which some threshold violation was found. The limits under consideration are according to the IEEE C37.118.1-2011 and its addendum IEEE C37.118.1a-2014 and considering only the limit rates of 60 SPF and 10 SPF, which are the more stringent. Tests not presented had results within the prescribed limits for both algorithms.

Results for the out-of-band rejection tests in the aforementioned tables are shown for the maximum allowable displacement from the nominal frequency, in other words, the worst case scenario. For the transmission rate $F_S = 60$ FPS this means $F_n = 63.0$ Hz, whereas for $F_S = 10$ FPS the frequency $F_n = 60.5$ Hz.

Table 2 presents the results for the band rejection tests, frequency ramp, and modulation for the transmission rate $F_S = 60$ FPS. In Table 3, results for the same tests are presented for $F_S = 10$ FPS. Results for the out-of-band rejection tests in the aforementioned tables are shown for the maximum allowable displacement from the nominal frequency, in other words, the worst case scenario. For the

transmission rate $F_S = 60$ FPS this means $F_n = 63.0$ Hz, whereas for $F_S = 10$ FPS the frequency $F_n = 60.5$ Hz.

Table 2: Test results for $F_S = 60$ FPS

Test	Algorithm 1			Algorithm 2			Limits (IEEE C37.118.1-1a)		
	TVE (%)	FE (mHz)	RFE (Hz/s)	TVE (%)	FE (mHz)	RFE (Hz/s)	TVE (%)	FE (mHz)	RFE (Hz/s)
Out-of-band	0,98	169,0	-----	0,02	5,2	-----	1,20	10,00	-----
Frequency ramp	0,32	11,0	0,35	0,10	0,1	0,01	1,00	10,00	0,20
Bandwidth (modulation)	0,82	140,0	11,00	0,09	45,0	1,50	3,00	300,00	14,00

Table 3: Tests results for $F_S = 10$ FPS

Test	Algorithm 1			Algorithm 2			Limits (IEEE C37.118.1-1a)		
	TVE (%)	FE (mHz)	RFE (Hz/s)	TVE (%)	FE (mHz)	RFE (Hz/s)	TVE (%)	FE (mHz)	RFE (Hz/s)
Out-of-band	0,71	17,0	-----	0,04	0,1	-----	1,20	10,00	-----
Frequency ramp	2,50	50,0	0,01	0,39	4,1	0,12	1,00	10,00	0,20
Bandwidth (modulation)	4,20	122,0	2,70	2,35	60,0	0,70	3,00	120,00	2,30

The values shown in yellow indicate violations of the standard limits. It is noticeable that most of the violations occur at the lowest rate (10 FPS) rather than at the highest rate (60 FPS), confirming that the lower transmission rates are the most demanding in terms of selectivity. Algorithm 1 meets the criterion of TVE for the band rejection test (OOB) in all rates, confirming its suitability for the previous version of the standard (IEEE C37.118-2005), which did not include dynamic tests. However, its selectivity is not good enough to meet the requirements of the new dynamic tests, especially in the case of bandwidth requirements for modulation tests.

Figure 5 presents a comparison of the gains of both algorithms in the upper frequency limit of the modulation test. The gain difference from 0.95 dB (Alg. 1) to 0.97 dB (Alg. 2) is sufficient to keep Algorithm 2 within the error limits for the TVE, FE and RFE across the entire range of the modulation frequency variation for all transmission rates.

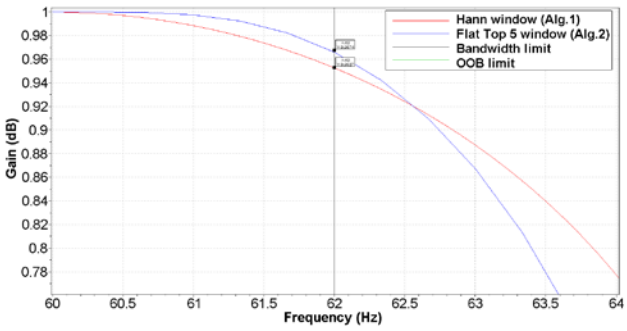

Figure 5: Comparison of Algorithms 1 and 2 gains for modulation test ($F_S = 10$ FPS)

At the same time, the higher attenuation presented by the Flat Top window at higher frequencies, in comparison to that of the Hann window (Figure 3), ensures compliance with the TVE and FE limits for the OOB test. Note that there are no RFE requirements for OOB.

With regards to the OOB test, it is worth mentioning that one should vary the nominal frequency of the signal by ± 10% of the Nyquist frequency of the transmission rate used during the test. For a nominal power system frequency of 60 Hz, at the rate of 60 FPS, the test should be conducted from 57 Hz to 63 Hz, and at the rate of 10 FPS, between 59.5 Hz and 60.5 Hz. As mentioned before, for algorithm 1 the instantaneous frequency is used to adjust the DFT window size. As a result, the frequencies above and below the nominal value used in the OOB tests shift the center of the window function and

therefore the gain at the test cutoff frequency. In Figure 6 a comparison of the spectra using the nominal frequency of 60 Hz and the limit of 60.5 Hz is shown.

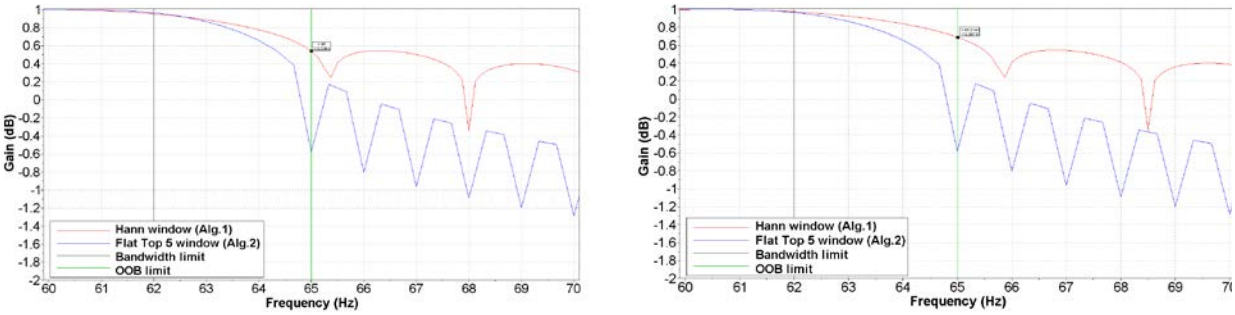

(a) f_N = 60 Hz (b) f_N = 60,5 Hz

Figure 6 - Spectrum in different nominal frequencies for the OOB test (F_S = 10 FPS)

As we can see, algorithm's 1 selectivity is degraded due to the adjustment of the window size by the instantaneous frequency. As shown in the chart, the gain increases from 0.53 dB to 0.69 dB in the OOB test limit, decreasing its band rejection capability. Algorithm 2, however, maintains its selectivity since it uses a fixed window and phasor compensation. As result, its TVE and FE errors remain below the limits even with a shift in the nominal frequency.

For the frequency ramp test, it is important to note that the use of lookup tables for the sines and cosines used in the DFT adjustment process of algorithm 1 also interfere with the accuracy of the results. 4000 entries were used in the range between 55 Hz and 65 Hz. For the rates of 20 SPF and 10 SPF, there is an integer number of points in the tables for each measurement step of the test (20 points at the rate of 20 FPS, and 40 points at the rate of 10 FPS), so that only exact values of sine and cosine are used during the frequency excursion of the input signal. For the other rates (60, 30, 15, and 12 FPS), the number of points in the tables is not round, so that at some measuring steps of the tests approximate values sine and cosine are used. This generates significant variations of consecutive frequency values in the rates of 60, 30, 15 and 12 FPS, which creates significant RFE. Algorithm 2, with a Flat Top window fixed in nominal frequency, does not suffer this influence.

5. CONCLUSIONS

This work aims to analyze the dynamic performance of PMU in accordance to tests and requirements of the latest version of IEEE synchrophasors standard. Two algorithms were implemented and analyzed. Algorithm 1 relies on a Hann window function with a window size adjustment based on the instantaneous frequency of the electrical system. Algorithm 2 was based on Flat Top 5 window function, with fixed windows size. Tests were performed using a hybrid simulation platform generating tests signals for a real PMU tests were the algorithms were implemented. It is worth noting that this test approach is more reliable than a purely theoretical approach, since it uses the algorithms of a real PMU.

It has been shown that algorithm 1, although able to meet the requirements of the previous version of the synchrophasors standard, which focused only static behavior, does not have enough performance to meet the dynamic requirements proposed in the recent versions of standard. In its turn, algorithm 2 meets all the performance requirements proposed in both the standard IEEE C37.118.1-2011 and its addendum IEEE C37.118.1a-2014.

The results indicated that the process window size adjustment, widely used in DFT based phasor calculation algorithms associated with a Hann window function, may cause degradation and loss of performance in some specific situations of the electric power system operation. The technique of fixed window size in used in algorithm 2, adjusting the modules and angles after the DFT calculation, proved more suitable face the dynamic requirements proposed in the standard.

It is noteworthy that the performance of the PMU algorithm should be all the better the smaller the phasor transmission rate. The limits of the band rejection tests (out-of-band interference) and

modulation are complementary and closer to one another in the frequency domain for lower rates, requiring greater selectivity of the algorithm. This brings to consideration the performance requirements that PMUs are subject for phasor computation at low transmission rates, in which the benefits of phasor measurement itself may not be fully realized. Currently, WAMS operating at rates higher than a frame per mains cycle have already been deployed for the monitoring of sub-synchronous resonance [12]. In [13] it is reported that torsional modes may reach 46 Hz (range of sub-synchronous frequencies), requiring PMUs with rates above the 60 FPS for a correct identification of such phenomena.

6. BIBLIOGRAPHIC REFERENCES

[1] AGOSTINI, M. N .; CRUZ, I. H .; Franzen T. A. et al. Merging Unit application for Synchronized Measurement Phasors. In: XII Protection and Control Technical Seminar - STPC. Rio de Janeiro, Brazil, November 2014.

[2] AGOSTINI, M. N .; ZIMATH, S .; ALVES JR., J. R. E. et al. Testing Agreement PMU IEEE Standard C37.118.1-2011. In: XXII National Seminar on Production and Transmission of Electricity - SNPTEE. Brasília, DF, October 2013.

[3] ALVES JUNIOR, J. E. R .; OLIVEIRA, S. C. G .; WATANABE, EH Analysis of Algorithms Internal Phasor Measurement Units. In: XI Protection and Control Technical Seminar - STPC. Florianópolis, November 2012.

[4] HEINZEL, G .; RÜDIGER, A .; SCHILLING, R. Spectrum and spectral density estimation by the Discrete Fourier Transform (DFT), including a comprehensive list of window functions and some new flat-top windows. In: Albert-Einstein-Institut. Hannover, February 2002.

[5] SALVATORE, L., TROTTA, A. Flat-top windows for PWM waveform processing via DFT. PROCEDINGS IEEE, vol. 135, Pt B, No. 6, November 1988.

[6] MedFasee project. (2015) [Online]. Available: http://www.medfasee.ufsc.br/

[7] DECKER, I. C .; AGOSTINI, M. N .; Dotta, D. et al. Development and Implementation of a Measurement System Prototype Synchronized Phasor in Transmission System of 440 KV CTEEP. In: XXI National Seminar on Production and Transmission of Electricity - SNPTEE. Florianópolis, SC, October 2011.

[8] ROSCOE, A. J .; Abdulhadi, I. F .; BURT, GM P-Class Phasor Measurement Unit algorithms using adaptive filtering to Enhance accuracy at off-nominal frequencies. Measurements for Future Smart Grids (SMFG), IEEE International Conference on Digital. doi: 10.1109 / SMFG.2011.6125761. November, 2011.

[9] IEEE Std. For Synchrophasor Measurements for Power Systems. IEEE Std C37.118.1-2011. December 2011.

[10] IEEE Std is Synchrophasor Measurements for Power Systems - Amendment 1:. Modification of Selected Performance Requirements. IEEE Std C37.118.1a 2014. March 2014.

[11] IEEE Guide for Synchronization, Calibration, Testing, and Installation of Phasor Measurement Units (PMUs) for Power System Protection and Control. IEEE Std C37.242 ™ -2013. March, 2013.

[12] ZIMATH, S .; WILSON, D .; AGOSTINI, M. N. et al. Novel Sub-Synchronous Oscillation Early Warning System for the GB Grid. In: Study Committee B5 Colloquium. Nanjing, China, September, 2015.

[13] PAL, B. Chaudhuri, B., Robust Control in Power Systems, Springer, 2005.